Relevance of Second Harmonic Generation Microscopy (SHG-M) in Material Sciences

Simon Clevers, Antoine Burel, Nicolas Couvrat, Valerie Dupray, Gérard Coquerel

Relevance of Second Harmonic Generation Microscopy (SHG-M) in Material Sciences

S. Clevers[1], A. Burel[1], N. Couvrat[1], V. Dupray[1*] and G. Coquerel[1]
[1]Laboratoire Sciences et Méthodes Séparatives, EA3233, Université de Rouen Normandie, 76821 Mont Saint Aignan, France.
*valerie.dupray@univ-rouen.fr

Second harmonic generation (SHG) is an extremely sensitive and rapid technique to detect absence of inversion centers in crystalline structures. Combined with microscopy, SHG-M, permits (i) to monitor temperature-induced phase transitions; (ii) to detect non-centrosymmetric zones inside heterogeneous materials. Therefore, as analytical tool, SHG-M covers a large domain of applications, in complement with other classical techniques (e.g. XRPD, DSC, optical microscopy). The present work illustrates the use of SHG-M in selected monophasic and multiphasic sample studies. Particularly, reinvestigation of Phenanthrene phase transition is presented.

1. Introduction

If an intense electromagnetic field (laser) interacts with a crystal, the dielectric polarization of this crystal is not a linear response of the incident electric field and new effects appear. Second harmonic generation (SHG) is a second-order non-linear optical effect which occurs in non-centrosymmetric crystals. The first observation of such phenomena was reported by Franken *et al.*[1] It should be noted that for centrosymmetric materials (i.e. where the inversion center is a symmetry element present in the crystal) second harmonic generation cannot occur. Among several methods to detect the noncentrosymmetry in crystals, SHG appears to be one of the most selective and sensitive because it allows the detection of almost all non-centrosymmetric classes[2] except the 432 classes. Note that for 622 and 422 classes SHG is theoretically forbidden by the Kleinman symmetry conditions. However, the Kleinman symmetry rule is only valid if there is no significant absorption, and thus presents some failures.[3] Consequently, if second-order nonlinear optical materials have attracted much attention due to their high potential for photonic and optoelectronic applications, especially as frequency doubling crystals or devices (such as photonic crystals) [4], SHG also appears to be relevant in systematic material analysis.[5] In 1968 Kurtz and Perry[6] developed a method for assessing the efficiency of SHG in powder samples. This method is of particular interest because suitable single crystals are often not available in many cases, and was widely used for large screening of materials where only a small amount of powder is required. Moreover, powder SHG (PSHG) measurements are extremely fast compared to other spectroscopic methods. PSHG has thus been used in many material studies, e.g. to (i) resolve space group ambiguities when X-ray methods failed to draw unambiguous conclusions (direct evidence of the presence or absence of centrosymmetry could be decisive) [7], (ii) find new efficient frequency converter crystals, and (iii) perform very fast pre-screening of conglomerate with relevant applications in the pharmaceutical industry[8] (the presence of a SHG signal often indicates the absence of racemic compound, a condition required for the application of Preferential Crystallization [9]). This method was also recently used to assess the structural purity of an organic compound down to the ppm level.[10] SHG can also be coupled with a heating stage to monitor solid-solid phase transitions (temperature-resolved SHG or TR-SHG). To date, this has been used in several works, with application to monotropic phase transition[11], enantiotropic phase transition[7] or order-disorder phase

transition [12]. It should be noted that the evolution of SHG signal with pressure was also recently studied[13].
Combined to a microscope, SHG microscopy (SHG-M) allows scientists to obtain a 2D or 3D view of the non-centrosymmetric zones (e.g. crystals, domains, defects) inside a bulk sample. SHG-M has proved a great relevance for imaging in several fields such as biology or material sciences. For example, SHG-M was used to monitor, in situ, the crystallization of a non-centrosymmetric phase from a supersaturated solution[14], to selectively detect the presence of a pharmaceutical compound inside an excipient matrix[15], to investigate microstructure[16], or to image a crystal undergoing a polymorphic transition[11].

Tab.1 Phenanthrene solid-solid phase transition data on heating, *under pressure (69MPa); [a]commercial, [c]see purification procedure in material and methods; [b]purification by sublimation and zone melting

Grade	sample	Technique	Onset (°C)	Peak (°C)	Enthalpy (J.mol^{-1})	Reference
98%[a]	powder	DSC	68.0	72.6	890	This work
Ultrapure[c]	powder	DSC	71.0	74.8	971	This work
90%[a]	Powder	SHG		65.0	-	This work
98%[a]	Powder	SHG		75.2	-	This work
Ultrapure[c]	Single- crystal	SHG		76.2	-	This work
98%[a]	powder	SHG	-	72 ±1	-	[7]
Purified[b]	powder	Calorimetry	62.4	72.8	1590	[17]
Purified[b]	Single-crystal	Calorimetry	-	-	1423	[17]
Purified[b*]	Powder	Resistivity	-	68	-	[18]
Purified[b]	Powder	Conductivity	-	74.3	-	[19]

PSHG, TR-SHG and SHG-M cover a large domain of applications as analytical apparatus in complement with other classical techniques (e.g. XRPD, DSC, optical microscopy). If non-centrosymmetric structures are not the most numerous among materials (e.g. 24.1% of the structures reported in the Cambridge Structural Database (CSD) are non-centrosymmetric [20]), they are preponderant in many fields of industrial applications (e.g. pharmaceuticals and optoelectronic devices).
Recently, we have successfully achieved the purification of phenanthrene with an ultimate purity of 99.999 mol%. We report herein the reinvestigation of the known phase transition of this compound by means of SHG-M.

2. Phase transition in phenanthrene.

Three polymorphs of phenanthrene are know: (i) a low temperature (LT) ordered form crystallizing in the $P2_1$ space group, (ii) a high temperature (HT) form crystallizing in $P2_1/c$ space group and exhibiting dynamic disorder and (iii) an additional high pressure polymorph crystallizing in the $P2_1/m$ space group.[21] In 1976, temperature-dependent SHG measurements were the first definitive evidence of the polymorphic transition between the LT-phase and the HT-phase (see Fig. 3a). [7] TR-SHG monitoring showed the progressive conversion of the LT form toward the HT on heating (complete vanishing of the SHG signal due to the inversion center symmetry element in HT-form), and electrical resistance measurements suggested the potential occurrence of two separate transitions of different orders in a narrow temperature range. Besides the unusual character of Phenanthrene solid-solid transition, another parameter was found to critically influence on the behavior of the compound in the solid state. Indeed, the chemical purity of the solid has a strong impact on the transition, as on the melting point of the compound. [22] This exemplified through the various data reported in the literature about the solid-solid phase transition and summarized in

Tab.1. They highlight, in particular, the discrepancies on the transition temperature and raised the question of the mechanism of the transition, which was, up to now, not resolved. The study of this transition by means of SHG-microscopy could help to understand or point out the microscopic mechanism.

2. Material and methods

2.1 Mulitphoton microscope and TR-SHG

Insight X3 single laser with automated dispersion compensation (Spectra-Physics, Santa Clara, USA) and a TCS SP8 MP confocal microscope (Leica Microsystems, Wetzlar, Germany) were used to performed confocal microscopy as well as two-photon microscopy imaging of the samples. The laser cavity had over 2.67 W of average power at 900 nm and was tunable from 680 nm to 1300 nm. The repetition rate was 80 MHz and the temporal width at the output of the cavity was around 120 fs (<100fs between 850 nm and 1050 nm). The laser was controlled with the LASX Leica software. Two Leica hybrid descanned detectors (HyD) were used to record images in backward direction. For two-photon imaging experiments, signal was collected after the microscope objective via a dichroic beamsplitter, transparent to wavelengths greater than 815 nm. Microscope objectives were long working distance dry Leica objectives (HC PL Fluotar 5X NA 0.15, HC PL Fluotar 10X NA 0.3 or HC PL APO 20X NA 0.4 CS2). An electro-optical modulator was used to adjust the laser power at the entrance of the confocal system. The spectral acquisition was performed using an internal hybrid detector. The collected photons were dispersed by a prism and a specific motorized split mirror selects the spectral detected band before the hybrid detector. Acquisitions were performed between 385 nm and 780 nm every 3 nm and a spectral bandwidth of 5 nm. In order to check if the sample produce fluorescence, an emission spectral scan is performed. Typically, the sample is excited at a given wavelength (*e.g.* 1200 nm or 900 nm) while scanned through the emission wavelength (*e.g.* in the 385nm-780nm range). The SHG and THG should appear at the half and at the third of the excitation wavelength, respectively. For temperature-resolved SHG measurements, the sample was placed in a computer controlled Heating-Cooling stage (Linkam THMS-600) having a 100ohm platinum resistor sensor DIN $1/10^{th}$ (maximum temperature deviation of 0.07°C in the 70°C-80°C range). The calibration of the Linkam was check by comparing melting temperature obtained by DSC and by the Linkam and was estimated at +/- 1°C A coverslide was placed on the top of the sample and gently pressed on it.

2.1 Differential Scanning Calorimetry (DSC)

Thermal analyses were conducted in a DSC 214 Netzsch equipped with an intra-cooler. The sample was placed in a 25-mL closed aluminum crucible. The atmosphere during the measurements was regulated by nitrogen flux ($50mLmin^{-1}$), and heating runs were conducted under conditions similar to those of the TR-SHG measurements in order to compare the results. Data treatment was performed with a Netzsch Proteus V.6.1

2.2 Ultra-purification of Phenanthrene

Different chemical grades (90% and 98%) of phenanthrene were purchased from Alfa Aesar. Ultrapure phenanthrene was obtained from 98% batch by combining different techniques as (i) Classical crystallization procedures (recrystallization in solution or from the melt), (ii) selective formation of co-crystals, (iii) selective chemical modification followed by a co-crystallization step, (iv) sublimation. In these work these pathways have been explored and a 99.999 mol.% ultimate purity of Phenanthrene has been achieved. Single-crystals of

phenanthrene was finally obtained by last sublimation operation. The mass of on typical single-crystal was estimated at circa 10µg.

3. Results and discussion

3.1 Effect of purification

In order to check the SHG efficiency of the phenanthrene, emission spectra of different phenanthrene grades (*i.e.* 90%, 98% and 99.999%) were recorded and are shown in Fig. 1. One can notice for all different grades, a sharp peak at 450 nm corresponding to the SHG signal (half of 900 nm excitation wavelength). Interestingly, both 90% and 98% grade exhibit emission spectra typical to fluorescence spectra but not for 99.999% grade. This behavior is probably closely related to the presence of impurities in phenanthrene although the emission spectra do not fit the emission spectra of the main impurities of phenanthrene (*i.e.* carbazole, dibenzothiophene, fluorene). One can recall that phenanthrene has the ability to form solid solutions with its impurities, consequently, the explanation for these particular emission spectra could be due to specific interactions in the solid state. This results point out the extreme sensitivity of confocal microscopy and the necessity to systematically check the purity of samples prior to experiments.

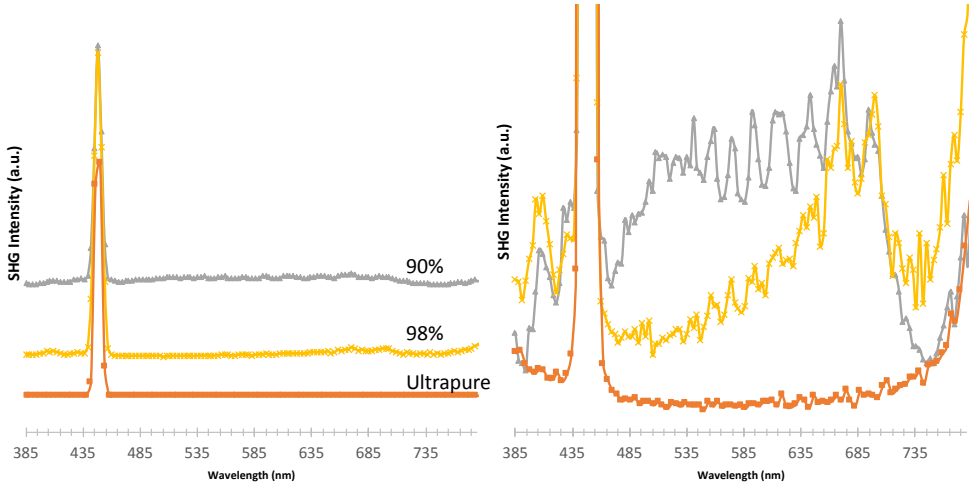

Fig. 1 Emission spectra of different phenanthrene grade for excitation wavelength at 900nm (left) and zoom in (right). The peak at 450 nm correspond to the Second harmonic emission.

3.2 Temperature resolved Second harmonic generation.

The phenanthrene has a propensity to sublimate. The sublimated sample could then recrystallized (from vapor) on the different optical elements (principally the fuse silica window of the heating/cooling stage). This could create unpredictable intensity fluctuation of the laser intensity arriving on the sample and misinterpretations. To limit such problems, and prior to TR-SHG experiment, the analyzed sample amount was reduced and a cover slide was place on the top of the sample to limit diffusion of molecules. For instance, for experiments concerning the ultrapure phenanthrene, a single-crystal of circa 10 µg was used.
The evolution of SHG with the temperature at 1K/min was monitored and different curves are presented in Fig. 3. For ultrapure phenanthrene, the signal disappears at 76.2°C (see **Erreur ! Source du renvoi introuvable.** and Fig. 3) In the historical SHG measurements, a 98% phenanthrene was used and the temperature was circa 72°C. If we assume that the commercial grade purity was similar in the 70's compared to the currently available commercial grade, this temperature is closely related to the DSC peak temperature (72.6°C) that correspond to end of the transition. The temperature of transition of ultrapure

phenanthrene found by SHG is much higher and could be due to a better detection threshold of the detector and a spectrally resolved analysis (avoiding misinterpretation). Nevertheless, transition temperature determined by SHG are 65°C and 75.2C for 90% and 98% phenanthrene grades, respectively. This highlights the crucial role of impurities in the phase transition. An increase of the impurities concentration creates a depression of transition point (more than 10°C between 90% and ultrapure grades).

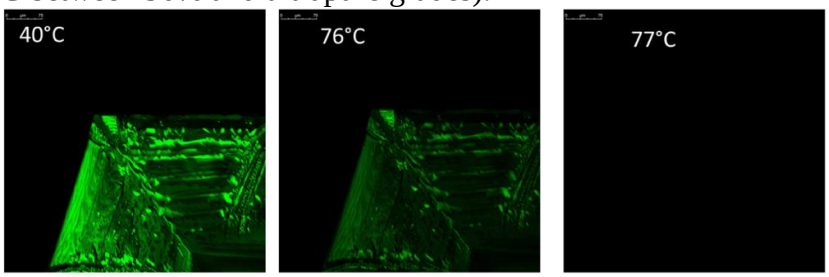

Fig. 2 SHG-M pictures upon heating of ultrapure phenanthrene single-crystal.

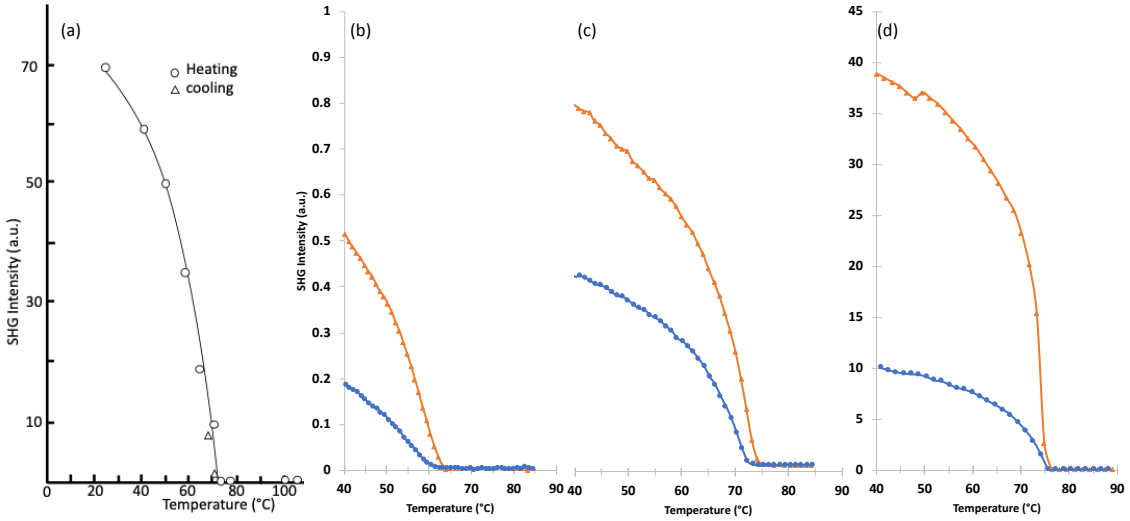

Fig. 3 TR-SHG curves of phenanthrene adapted from [7] (a) and for 90% (b), 98% (c) and ultrapure (d) grades.

The impurities concentration seems not drastically changed the unusual character of the transition observed in the SHG measurements. The LT-form still seems undergoing a progressive transition toward the HT-form. One can also notice the hysteresis in the appearance/disappearance temperature of the SHG signal upon cooling/heating increases with the impurities concentration (0.5°C, 2.8°C and 4°C for the ultrapure, 98% and 90% phenanthrene grades, respectively). In addition to observed peak in DSC, this clearly proves the 1st order contribution of this transition. Fig. 3(b-d) shows that the SHG intensity on cooling is lower compare to that upon heating. This could be due to stress induce by thermal treatment and solid-solid transition in the crystals. In addition, for temperature cycle experiment the SHG intensity upon cooling is (i) higher if the temperature of transition is not exceeded (*e.g.* cycle from 50°C to 65°C), (ii) lower if the temperature of transition is exceeded. Further investigations are in progress to understand such behavior.

Conclusion

The solid-solid transition of phenanthrene sample of different purity grades was investigated by means of SHG-M. Influence of impurities was highlighted. The impurity concentration do not change the progressive transition from the LT to the HT form observed in SHG but has drastic influence on the temperature of transition and hysteresis. Further investigations are in progress to understand the behavior observed during temperature cycles.

References

[1] P. A. Franken, A. E. Hill, C. W. Peters, and G. Weinreich, “Generation of Optical Harmonics,” *Phys. Rev. Lett.*, vol. **7**, pp. 118–119, Aug. 1961.

[2] K. M. Ok, E. O. Chi, and P. S. Halasyamani, “Bulk characterization methods for non-centrosymmetric materials: second-harmonic generation, piezoelectricity, pyroelectricity, and ferroelectricity,” *Chem. Soc. Rev.*, vol. **35**, no. 8, p. 710, 2006.

[3] D. A. kleinman, “Theory of Second Harmonic Generation Light,” *Physical Review*, vol. **128**, no. 4, pp. 1–15, Nov. 1962.

[4] A. Arie and N. Voloch, “Periodic, quasi-periodic, and random quadratic nonlinear photonic crystals,” *Laser & Photon. Rev.*, vol. **4**, no. 3, pp. 355–373, Apr. 2010.

[5] J. H. Richardson, *Systematic Materials Analysis*. Elsevier, 1978.

[6] S. K. Kurtz and T. T. Perry, “A Powder Technique for the Evaluation of Nonlinear Optical Materials,” *J. Appl. Phys.*, vol. **39**, no. 8, pp. 3798–3813, 1968.

[7] J. P. Dougherty and S. K. Kurtz, “A second harmonic analyzer for the detection of non-centrosymmetry,” *J Appl Crystallogr*, vol. **9**, no. 2, pp. 145–158, Apr. 1976.

[8] A. Galland, V. Dupray, B. Berton, S. Morin-Grognet, M. Sanselme, H. Atmani, and G. coquerel, “Spotting Conglomerates by Second Harmonic Generation,” *Crystal Growth & Design*, vol. **9**, no. 6, pp. 2713–2718, Jun. 2009.

[9] G. coquerel, “Preferential Crystallization,” in *Supramolecular chirality*, vol. **269**, no. 77, M. Crego-Calama and D. N. Reinhoudt, Eds. Berlin, Heidelberg: Springer Berlin Heidelberg, 2006, pp. 1–51.

[10] S. Clevers, F. Simon, V. Dupray, and G. coquerel, “Temperature resolved second harmonic generation to probe the structural purity of m-hydroxybenzoic acid,” *Journal of Thermal Analysis and Calorimetry*, no. 112, pp. 1–7, 2013.

[11] S. Clevers, F. Simon, M. Sanselme, V. Dupray, and G. coquerel, “Monotropic Transition Mechanism of m-Hydroxybenzoic Acid Investigated by Temperature-Resolved Second Harmonic Generation,” *Crystal Growth & Design*, vol. **13**, no. 8, pp. 3697–3704, Jul. 2013.

[12] L. Yuan, S. Clevers, A. Burel, P. Negrier, M. D. Barrio, B. Ben Hassine, D. Mondieig, V. Dupray, J. L. Tamarit, and G. coquerel, “New Intermediate Polymorph of 1-Fluoro-adamantane and Its Second-Order-like Transition toward the Low Temperature Phase,” *Crystal Growth & Design*, vol. **17**, no. 6, pp. 3395–3401, May 2017.

[13] Bayarjargal and Winkler, “Second harmonic generation measurements at high pressures on powder samples,” *Zeitschrift für Kristallographie – Crystalline Materials*, vol. **229**, no. 2.

[14] D. J. Kissick, D. Wanapun, and G. J. Simpson, “Second-Order Nonlinear Optical Imaging of Chiral Crystals,” *Annual Review of Analytical Chemistry*, vol. **4**, no. 1, pp. 419–437, Jul. 2011.

[15] S. J. Toth, J. T. Madden, L. S. Taylor, P. Marsac, and G. J. Simpson, “Selective Imaging of APIs in Powdered Blends with Common Excipients Utilizing TPE-UVF and UV-SONICC,” *Anal. Chem.*, vol. **84**, no. 14, pp. 5869–5875, Jul. 2012.

[16] H. Yokota, J. Kaneshiro, and Y. Uesu, “Optical Second Harmonic Generation Microscopy as a Tool of Material Diagnosis,” *Physics Research International*, vol. **2012**, no. 7, pp. 1–12, 2012.

[17] R. A. Arndt and A. C. Damask, “Heat-Capacity Anomaly in Phenanthrene,” *J. Chem. Phys.*, vol. **45**, no. 2, pp. 755–756, Jul. 1966.

[18] P. A. Andrews, A. F. Armington, and B. Rubin, “An Anomaly in the Resistivity-Temperature Profile of Ultrapure Phenanthrene,” *Applied Physics Letters*, vol. **7**, no. 4, pp. 86–88, Aug. 1965.

[19] R. A. Arndt and A. C. Damask, “Conductivity and Polarization Phenomena in Phenanthrene Crystals,” *J. Chem. Phys.*, vol. **45**, no. 12, pp. 4627–4633, Dec. 1966.

[20] F. H. Allen and W. Motherwell, “Applications of the Cambridge Structural Database in organic chemistry and crystal chemistry,” *Acta Crystallographica Section B*, **B58**, pp 407-422, 2002.

[21] V. Petricek, I. Císařová, L. Hummel, J. Kroupa, and B. Brezina, “Orientational disorder in phenanthrene. Structure determination at 248, 295, 339 and 344 K,” *Acta Crystallogr B Struct Sci*, vol. **46**, no. 6, pp. 830–832, Dec. 1990.

[22] N. Couvrat, A. Burel, S. Tisse, Y. Cartigny, and G. coquerel, “Combining zone melting and preparative chromatography to purify Phenanthrene,” *Journal of Thermal Analysis and Calorimetry*, vol. **112**, no. 1, pp. 293–300, Oct. 2012.

Aknowledgment

This work has been funded by Region Normandie and the *European Regional Development Fund* (FEDER-FSE Normandie 2014-2020) through the project SCAMPI